ASSESSMENT OF SHADOW INDEX USING RAY TRACING BASED ON A VOXEL MODEL ON VARIOUS STRUCTURES

Takumi Fujiwara (1), Wataru Takeuchi (2)
Institute of Industrial Science, The University of Tokyo, 4-6-1 Komaba, Meguro-ku,
Tokyo, 153-8505, Japan
Email: ftakumi@iis.u-tokyo.ac.jp; wataru@iis.u-tokyo.ac.jp

KEY WORDS: Forest, Direct irradiance, Scattering irradiance, Shade

ABSTRACT: Based on radiance which was sensed by sensor attached on satellite, many science institutes and researchers has developed some indices or products to monitor environment of the earth. However, index which shows structure of a forest is few. One of the index to estimate forest structure is shadow index (SI). To evaluate accuracy of SI, model which can represent complexity of forest structure was needed. Moreover, using the model, inversely estimation of radiance was needed. So we focused on a voxel model which can represent complex structures of a forest. In this research, we developed a ray tracing method using a voxel model. Test area was selected evergreen broad-leaved forests and evergreen needle-leaved forest. Target satellite image was Sentinel. Firstly, point cloud of test area was acquired. Secondly voxelize point cloud. Thirdly shadow and shade was calculated in each voxel. Finally, SI was simulated from voxel model (SIV) and compared Sentinel SI. From the result of correlation analysis of SI and SIV, it was found that the correlation coefficient on pixel which the difference of maximum and minimum of SI on annual was over about 2 was over 0.8. Additionally, in order to assessed SI, we used rumple index. Rumple index is useful index to show complexity of forest structure. The result of correlation analysis of SI and rumple index, it was found that the correlation coefficient increases as the solar zenith angle decreases. Using the proposed ray tracing method, we can expect inverse estimation of various vegetation indices as well as SI. However, the accuracy of the ray tracing method was about 0.6 on evergreen broad-leaved forest and about 0.7 on evergreen needle-leaved forest. For future task, firstly, to improve accuracy of the ray tracing method, it is necessary to consider the influence of BRDF function and environmental illumination. Secondly, inverse estimate various vegetation indices and investigate how sensitive the vegetation indices are to the structure of the forest. Investigating the relationship between some vegetation indices and forest structure, contribute to estimating three dimensional model could from satellite image.

1. INTRODUCTION

1.1. Background

With improving of sensor ability mounted on satellite, spatial resolution and spectral resolution being higher than before that. Based on radiance which was sensed by sensor attached on satellite, many science institutes and researchers has developed some indices or products to monitor environment of the earth. In particular, since amount of biomass or leaf area is important parameter of various ecosystem models (Running and Coughlan, 1988) (Ito and Oikawa, 2002) (Krinner et al., 2005). Indices which related to forest is many. Normalized difference vegetation index (NDVI) is famous index. The index can highlight the area of vegetation. So using the index, anyone can classify land cover or tree species and estimate leaf area using vegetation indices. However, index which shows three dimensional structure of a forest is few.

Ono et al., (2007) developed new vegetation index called shadow index (SI). Moreover, Ono et al., (2015) examined about relationship between SI and height of tree using MODIS. The result showed that SI is higher accuracy to estimate canopy height than other vegetation index. Therefore, using SI, estimation for above ground biomass will be expected. To verify useful SI, more detail examination is needed.

To evaluate SI that was affected by differences of three dimensional structure of a forest, inverse estimation method for radiance is needed that ray tracing using physical model. The physical model is combined atmosphere and land cover. Usually, forest model which combined simple shaped tree such as cylinder, spheroid and cone was used as land cover (Kobayashi et al., 2008). But, in many cases, the model can't represent complex structure of a forest. Voxel model is one suitable model that can represent complex structures of a forest. In this research,

1.2. Objective

The objective of this research is to develop a ray tracing method using a voxel model and assessment of SI by it.

Firstly, we explain about ray tracing using a voxel model. To verify accuracy of this method, we used aerial photographs taken by Unmanned Aerial Vehicle (UAV). Radiation emittance for target forest was simulated and it was evaluated that correlation coefficient of simulated radiant emittance and digital number of red band of aerial photographs. In this research, only direct irradiance and diffuse irradiance was target. The reason for comparing with red band is avoid the influence of Rayleigh scattering as much as possible. Test areas were selected evergreen broad-leaf forests and evergreen needle-leaf forest. Secondly, we assessed SI. SI was compared with rumple index (canopy surface area/ground surface area) and SI simulated by voxel model (SIV).

2. METHODOROGY

2.1. Development of ray tracing using a voxel model

As shown in the Figure 1, sensors mounted satellite or cameras mounted UAV observes reflected sunlight from features. Hence, if we could know camera position, camera orientation, sunlight spectrum and 3d structure of forest, aerial photograph will be simulated.

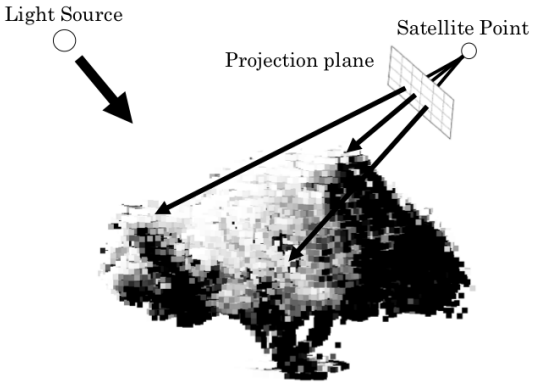

Figure 1. Diagram of ray tracing using voxel model

To simulate of radiant emittance by ray tracing, firstly, direct irradiance and scatter irradiance was calculated using SMARTS_295. SMARTS_295 is a free soft and output direct irradiance (L_{dir}) and scatter irradiance (L_{dif}) to input date, location and atmospheric parameters. Targeting for leaved tree, digital number of red band (R) is given as Equation 1. In this research, reflectance of leaf and stem was not considered because we used correlation coefficient instead of error to evaluate accuracy. Accurate wavelength range of red band of aerial photograph is unknown. Therefore, in this research, we define wavelength range of red band is 580nm to 620nm. In that wavelength range, irradiance was output used SMARTS_295.

$$R \propto L_{dir}(1 - Shadow) + L_{dif}Shade \quad (1)$$

2.2. Calculate shadow and shade

Firstly, point cloud was acquired by SfM (Structure from Motion) using aerial photographs. SfM software is PhotoScan (Agisoft PhotoScan Professional Ver.1.4.4). Point cloud outputted has XYZ coordinate and normal vector as attribute. Secondly, voxelize point cloud. The voxel size is 10 cm. Each voxel has average XYZ coordinate and normal vector as attribute. Thirdly, shadow proportion was calculated in each voxel from the positional relationship of each voxel and sun. Finally, image was simulated by collinear conditional expression using camera location, Internal orientation and external orientation output from PhotoScan.

Shadow indicates the area ratio where the voxel is blocked from the sun by other voxels. However, it is difficult to accurately calculate the area where light is blocked. In this study, by considering the calculation of shadow as follows, we aimed to reduce the calculation cost. Firstly, a plane parallel to the XY plane was assumed at the average Z coordinate position of the voxel. Secondly, the plane was divided into four and a line is generated from each plane toward the sun. Finally, among the four straight lines, the shadow ratio was determined by the number of lines intersecting the plane of other voxels. In other words, the shadow proportion is either 0.0, 0.25, 0.5, 0.75, 1.0. For example, in case of Figure 2, shadow is 0.75.

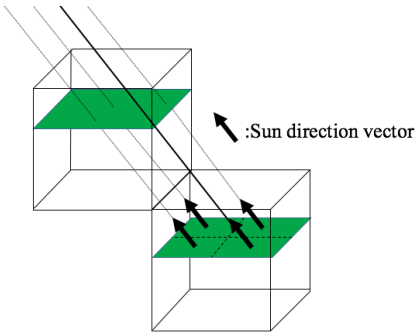

Figure 2. Diagram of shadow calculation

Ordinary, Phong reflection model (Phong, 1975) was used for calculate shade. This model calculates the cosine of the angle formed by the normal vector of the object and the direction vector toward the light source. However, this method was considered effective when applied to a model assuming a smooth continuous surface, but not when applied to a model that mimics the actual forest surface. Therefore, we calculate Sky view factor (Svf) (Dozier and Frew, 1990) shown Equation 2 instead of cosine.

$$\mathrm{Svf} = \frac{1}{2\pi}\int_0^{2\pi}\left[\cos S \sin H_\phi + \sin S \cos(\phi - A)\,(H_\phi - \sin H_\phi \cos H_\phi)\right] d_\phi \qquad (2)$$

Where S means inclination angle and A means inclination direction at point targeted. H_φ means angle from zenith to horizon of direction φ. Iikura et al., (2003) calculated horizontal line H_φ by using DEM (Digital Elevation Model) to discretize the azimuth and calculated the contents of the integral of the Equation 2. In this study, the contents of the integral of the Equation 2 was calculated using the Z coordinate stored in image. Iikura et al., (2003) discretized the direction to 64 directions, but we discretized it to 8 directions.

2.3. Test area

Figure 3 shows test area to verify accuracy of ray tracing proposed. Evergreen broad-leaved forest targeted located on called Saoka District and evergreen needle-leaved forest targeted on called Matuo pass. These forests located at Kochi prefecture in Japan. Table 1 shows the geometric accuracy of each area. Verification point on Saoka District is P2 and Matuo Pass is M-4. Maximum error of each point is 6.40cm and 1.79cm.

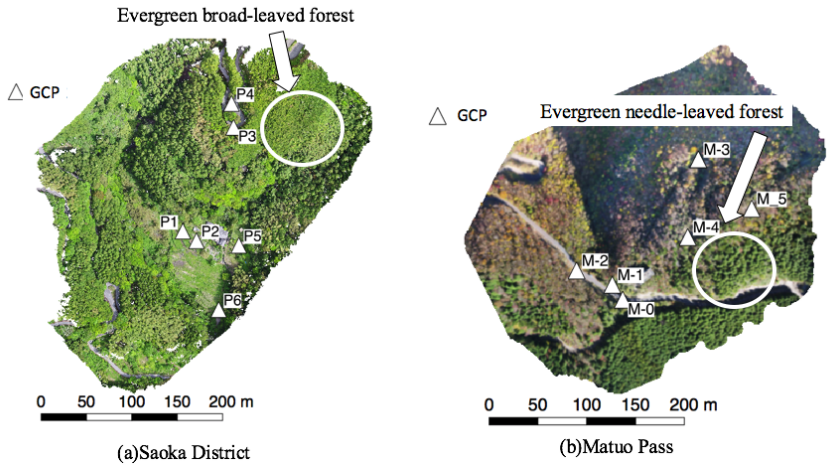

Figure 3. Test forest of evergreen broad-leaved forest and evergreen needle-leaved forest

Table 1. Geometric accuracy of point cloud on Saoka District and Matuo Pass

Saoka District	X(cm)	Y(cm)	Z(cm)	XY(cm)	Total(cm)
P1,P3,P4,P5,P6	3.01	2.00	2.33	3.62	4.30
P2	6.40	5.12	1.29	8.20	8.30

Matuo Pass	X(cm)	Y(cm)	Z(cm)	XY(cm)	Total(cm)
M-0,M-1,M-2,M-3,M-5	0.88	3.20	4.67	3.32	5.73
M-4	1.31	1.76	1.79	2.20	2.84

2.4. Accuracy assessment method

We assessed SI using voxel model. Figure 4 shows the flow of data processing. SI was defined as Equation 3. To assess SI, Rumple Index (canopy surface area/ground surface area) and shadow index simulated by voxel model (SIV) was used. Simulate target image was Sentinel. Band used is B4, B5, B6, B7, B8, B8A, B11 and B12. Spatial resolution was 20m.

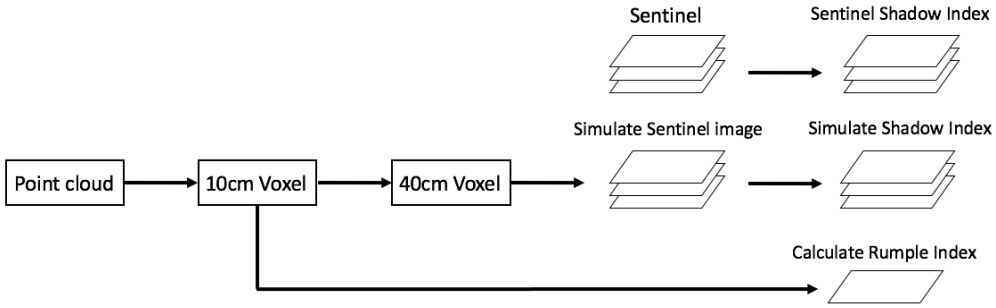

Figure 4. Flow chart of data processing to assess SI

$$SI = \frac{1}{\frac{1}{N}\sum_{j=1}^{N} r_j} \tag{3}$$

Here, r_j is the apparent reflectance of band i and N is the number of bands.

3. RESULT AND DISCUSSION

3.1. Validation of ray tracing accuracy

Point cloud of evergreen broad-leaved forest was obtained at April 23th, 2018, and point cloud of evergreen needle-leaved forest was obtained at October 25th, 2018. The density of point cloud was 1 point / 10^3cm^3. Each target image and simulate image was shown Figure 5. These images resolution are 10cm. Figure 5 is scatter plot graph of simulated emittance and digital number of red band taken from UAV. Scatter plots were created by down-sampling each image to 50 cm, 100 cm, 150 cm, and 200 cm.

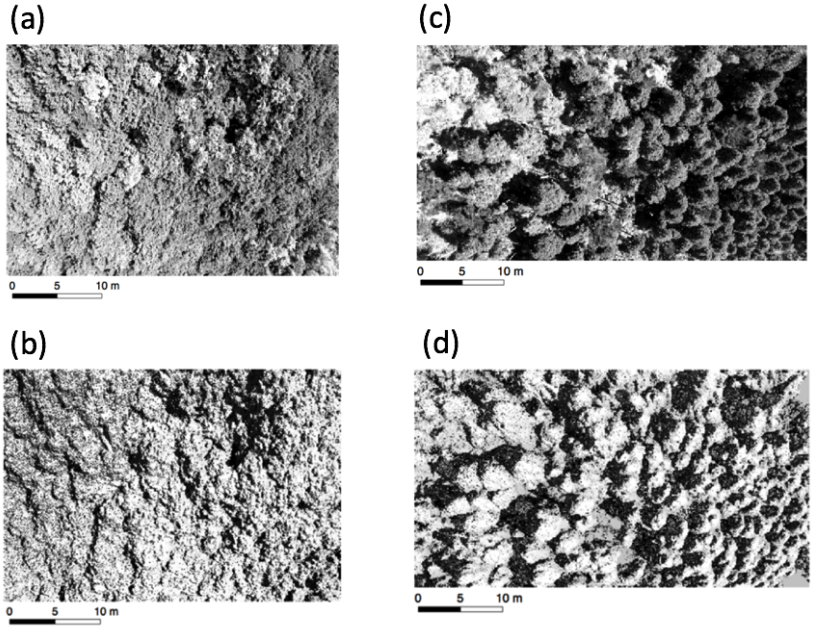

Figure 5. Target photograph of evergreen broad-leaved forest (a) and simulated image (b). Target photograph of evergreen needle-leaved forest (c) and simulated image (d).

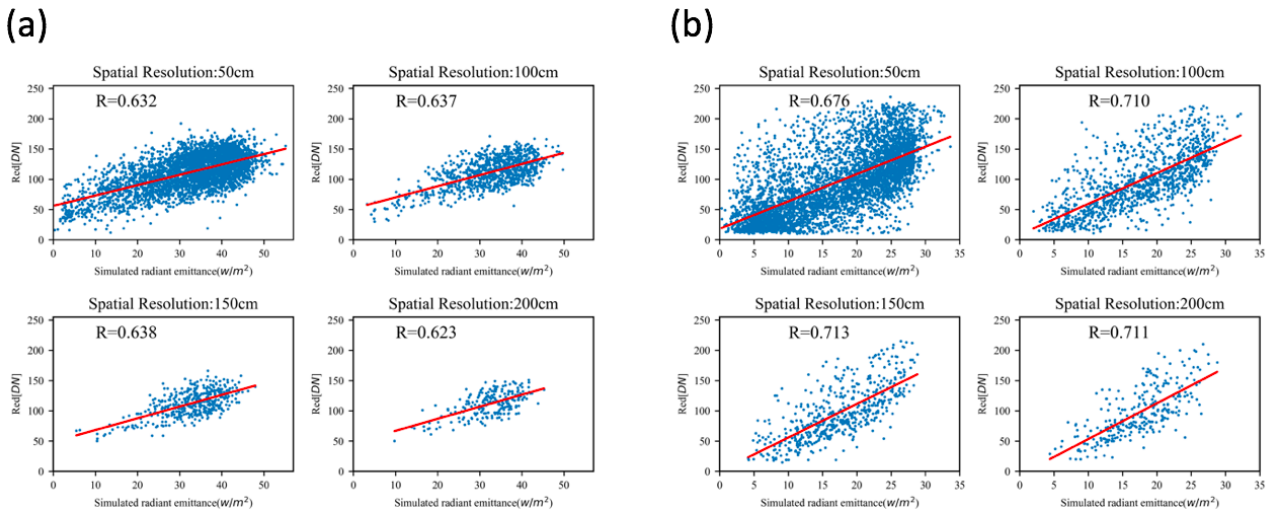

Figure 6. Simulation accuracy of ray tracing using voxel model in each resolution on evergreen broad-leaved forest (a) and evergreen needle-leaved forest (b)

From Figure 6, it was found that correlation coefficient on evergreen broad-leaved forest is over 0.6 and evergreen needle-leaved forest is over 0.7 in each resolution. Although the correlation coefficient was expected to increase as the resolution was lowered, there was little change in the correlation coefficient when the resolution was lower than 100 cm.

3.2. Relationship between SI and roughness of a forest surface

Kane et al., (2008) examined relationship between rumple index and stand characteristics such as shadow proportion at various solar zenith angles, mean diameter at breast height. The results showed high correlation of these relationship. Several other studies have examined the relationship between the rumple index and the complexity of canopy (Kane et al., 2010) (Yoga et al., 2017). Therefore, rumple index is useful index to show complexity of forest structure. Hence, in order to evaluate the relationship between SI and the structure of forest, the correlation between rumple index and SI was examined. Target area was Saoka.

Firstly, since point cloud density was 1 point / $10^3 cm^3$, we assumed surface area of each voxel was $10cm^2$. Secondly, total surface area per pixel was calculated and it was divided ground surface area. Finally, SI of the date shown in Table 2 was calculated, and each SI was compared with rumple index.

Table 2. Date of Sentinel images used and correlation coefficient of rumple index and SI

Date	Sun Azimth	Sun Zenith	R
01/24/2018	157.105	56.428	0.360
02/23/2018	152.356	47.85	0.431
03/10/2018	150.094	42.308	0.457
04/19/2018	141.903	27.459	0.540
05/19/2018	130.414	20.128	0.568
05/24/2018	128.168	19.464	0.590
07/13/2018	121.592	20.219	0.604
08/17/2018	136.751	26.168	0.544
10/21/2018	161.830	46.214	0.428
11/25/2018	164.412	56.104	0.336
11/30/2018	164.242	57.069	0.324

From Table 2, it was found that the correlation coefficient tended to increase as the solar zenith angle decreased. The trend is similar to the results of Kane et al., (2008). The Sentinel image in June could not be used due to the large number of clouds, but it is expected that the correlation coefficient will increase due to the smallest zenith angle. In other words, the June image is considered suitable for estimating the rumple index from the Sentinel image using SI.

3.3. Relationship between SI and simulated SI

Since the ray tracing method proposed in this study does not consider atmospheric effects, the absolute value of SI couldn't be estimated. Therefore, SIV was not compared with SI at one season but analyzed the correlation with SI at multiple seasons (shown Table 2).

Firstly, voxel size was converted 40cm. From the results in Chapter 2, we can see that when aerial images were simulated using our proposed method, the resolution was about 0.6 at each resolution. However, it is necessary to understand the resolution of the voxel model suitable for simulation according to the spatial resolution of the target satellite image. Therefore, this time, we set the voxel size to 1/50 of the target resolution, referring to the results of Sugino et al., (2016). Sugino et al., (2016) studied the resolution of Digital Surface Model (DSM) suitable for satellite image simulation. The result showed that 1/50 resolution of the target image is suitable. Although we used voxel model not DSM, we referenced their study result. Secondly, the reflectance of Betula (Noda et al., 2014) was inputted in each voxel attribute. The input reflectance should have been measured in the target area. However, since forest structure was focused, it was considered that an accurate reflectance was unnecessary. Finally, SI in each season was simulated. Target area was Saoka.

Figure 7 shows the correlation coefficient of SI and VSI on each pixel. From Figure 7, the correlation coefficient is not constant on all pixels but difference. In particular, it can be seen that the correlation tends to was low in evergreen broad-leaved forests. To clearly the characteristic, Figure 8 shows the scatter plots of difference of maximum and minimum of SI and correlation coefficient. From Figure 8, it was found that the correlation coefficient on pixel which the difference was over about 2 is over 0.8. Therefore, on the pixel which the difference of its over 2, seasonal change of SI was depended on shadow caused by changes in the solar position.

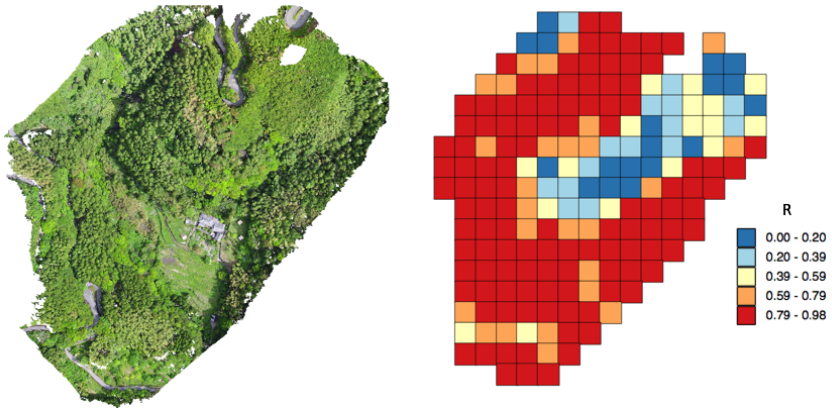

Figure 7. Correlation coefficient of SI and SIV on each pixel

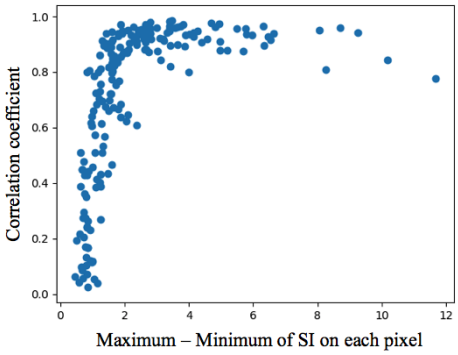

Figure 8. Relationship of the difference of maximum and minimum of annual SI and correlation coefficient

4. CONCLUSION

In this study, we proposed a ray tracing method using voxel model and assessed SI. The accuracy of ray tracing was verified by correlation coefficient of red band image taken by UAV and radiant emittance simulated. Since the exact red band wavelength range was unknown, the radiant divergence in the approximate wavelength range was simulated. Firstly, aerial images with resolution of 10 cm were simulated from a voxel model with a size of 10cm. Next, image resolution was downsampled to 50cm, 100cm, 150cm and 200cm. Finally, correlation coefficient of simulated images

and aerial images was calculated in these resolution. Result shows that correlation coefficient was over 0.6 on evergreen broad-leaved forest and 0.7 on evergreen needle-leaved forest. To improve accuracy, it is necessary to consider the influence of Bi-directional Reflectance Distribution Function (BRDF) and environmental illumination.

In order to assessed SI, we used rumple index and SIV. The result of correlation analysis of SI and rumple index, it was found that the correlation coefficient increases as the solar zenith angle decreases. Hence, the June image is considered suitable for estimating the rumple index from SI of Sentinel image. The result of correlation analysis of SI and SIV, it was found that the correlation coefficient on pixel which the difference was over about 2 is over 0.8. Therefore, on the pixel which the difference of its over 2, seasonal change of SI was depended on shadow caused by changes in the solar position.

Using the proposed ray tracing, we can expect inverse estimation of various vegetation indices as well as SI. Future tasks are to inverse estimate various vegetation indices and investigate how sensitive the vegetation indices are to the structure of the forest.

5. REFERENCE

Bui, T. P., 1975. Illumination for computer generated pictures, Communications of the ACM, 18(6), pp.311-317

Dozier, J., Frew, J., 1990. Rapid calculation of terrain parameters for radiation modeling from digital elevation data, IEEE Transactions on Geoscience and Remote Sensing, 28(5), pp.963-969

Iikura, Y., Saito H., Tanba S., 2003. Correction of Topographic Effects in Satellite Images with Due Consideration on Spatial Variation of Irradiance, Journal of The Remote Sensing Society of Japan, 23(4), pp.386-392

Ito, A., Oikawa T., 2002. A simulation model of the carbon cycle in land eco-systems (Sim-CYCLE): A description based on dry-matter production theory and plot-scale validation, Ecological Modelling, 151, pp.143-176

Kane, V., Gillespie, A., Mcgaughey, R., Lutz, J., Ceder, K., Franklin, J., 2008. Interpretation and topographic compensation of conifer canopy self-shadowing. Remote Sensing of Environment. 112. pp.3820-3832.

Kane, V., Mcgaughey, R., Bakker, J., Gersonde, R., Lutz, J., Franklin, J., 2010. Comparisons between field- and LiDAR-based measures of stand structural complexity. Canadian Journal of Forest Research. pp.761-773

Kobayashi, H., Iwabuchi, H., 2008. A coupled 1-D atmosphere and 3-D canopy radiative transfer model for canopy reflectance, light environment, and photosynthesis simulation in a heterogeneous landscape, Remote Sensing of Environment, 112(1), pp.173-185

Krinner, G., Viovy, N., de Noblet-Ducoudre, N., Ogee, J., Polcher, J., Friedlingstein, P., Ciais, P., Sitch, S., Prentice, I, C., 2005. A dynamic global vegetation model for studies of the coupled atmosphere-biosphere system, GLOBAL BIO-GEOCHEMICAL CYCLES, 19, GB1015

Noda, H., Motohka, T., Murakami, K., Muraoka, H., Nasahara, K., 2014. Reflectance and transmittance spectra of leaves and shoots of 22 vascular plant species and reflectance spectra of trunks and branches of 12 tree species in Japan, Ecological Research, 29(2), pp.111

Ono, A., Kajiwara, K., Honda, Y., Ono, A., 2007. Development of vegetation index using radiant spectra normalized by their arithmetic mean. Proceedings of the 2007 Asian Conference on Remote Sensing, PS3.G6.5.

Ono, A., Takeuchi, W., Hayashida, S., 2015. Estimation of forest canopy height using MODIS shadow index. Proceedings of the 2015 Asian Conference on Remote Sensing, TU4.1.6

Running, S. W., Coughlan, J. C., 1988. A general model of forest ecosystem processes for regional applications, I. Hydrologic balance, canopy gas exchange and primary production processes, Ecological Modeling, 42, pp.125-154

Sugino, K., Takagi, M., 2016. Ground sampling distance of Digital Surface Model for Land Observation Satellite Data Analysis, Journal of the Japan Society of Photogrammetry, 55(3), pp.191-199

Yoga, S., Bégin, J., St-Onge, B., Riopel, M., 2017. Modeling the Effect of the Spatial Pattern of Airborne Lidar Returns on the Prediction and the Uncertainty of Timber Merchantable Volume. Remote Sensing, 9, pp.808